Multi-stage pseudomorphic replacement of garnet during polymetamorphism: 2. Algebraic analysis of mineral assemblages

B. CESARE
CNR Centro di Studio per la Geodinamica Alpina, and Dipartimento di Mineralogia e Petrologia – Università di Padova, Corso Garibaldi 37, I-35137 Padova, Italy (bernardo@dmp.unipd.it)

ABSTRACT Chemical relationships among four metapelites have been studied by investigation of mineral and bulk chemistry data and by singular value decomposition analysis of single and composite assemblage matrices. Bulk rock compositions cluster close together in an AFM diagram, all within the intersection space defined by the four sample assemblages. The similarity of bulk compositions normalized on a silica-free, anhydrous basis indicates that sample chemistries differ mainly as a result of inhomogeneous distribution of quartz layers. The existence of mass balance relationships among samples indicates that assemblages also overlap in the Si–Ti–Al–Fe–Mg–Mn–Ca–Na–K multisystem. Analysis of single and composite matrices helps in defining possible mass balances linking sample mineral facies to one another during progressive contact metamorphism. The assemblage in sample A can form as the result of the model reaction

$$5.000\ \mathrm{Ky} + 0.269\ \mathrm{Grt} + 0.965\ \mathrm{Bt} + 0.314\ \mathrm{Pl} = 0.049\ \mathrm{Ilm} + 1.115\ \mathrm{Ms} + 0.849\ \mathrm{Chl} + 0.306\ \mathrm{St}$$

and react to assemblage B via reaction

$$0.97\ \mathrm{Chl} + 0.52\ \mathrm{Grt} + 0.66\ \mathrm{Ms} + 0.14\ \mathrm{Ilm} + 1.26\ \mathrm{Ky} = 0.42\ \mathrm{St} + 0.63\ \mathrm{Bt} + 0.22\ \mathrm{Pl}$$

coupled with the Ky→And transition. Assemblage B can transform into C by initial progress of

$$\mathrm{Ky} + \mathrm{Ilm} + \mathrm{Chl} + \mathrm{Grt} + \mathrm{Ms} = \mathrm{And} + \mathrm{St} + \mathrm{Bt} + \mathrm{Pl}$$

followed by

$$0.142\ \mathrm{Ilm} + 0.175\ \mathrm{St} + 1.089\ \mathrm{Chl} + 1.533\ \mathrm{Ms} + 0.003\ \mathrm{Grt} = 5.000\ \mathrm{And} + 1.266\ \mathrm{Bt} + 0.551\ \mathrm{Pl}$$

Matrix analysis cannot satisfactorily model the C–D transition, because it predicts a net production of staurolite, which is in disagreement with petrographic evidence. All mass balances in the C–D composite matrix indicate net consumption of muscovite; this is integrated with the contrasting evidence of prograde pseudomorphs of muscovite after staurolite, observed in the nodules of sample D, within a model involving the progress of ionic reaction cycles.

Key words: algebraic analysis; mass balance; metamorphic reaction; metapelite; SVD technique.

INTRODUCTION

Comparison of rock samples along a metamorphic traverse or within a single outcrop leads to the necessity of determining whether different mineral assemblages are the result of changes in intensive parameters of metamorphism (e.g. P, T, a_{H_2O}) or could have equilibrated at the same metamorphic conditions, due to variations in bulk composition. Such a determination may be made by analysing mass balance relationships among a pair of assemblages: if a mass balance exists, the assemblages did not equilibrate at the same metamorphic conditions; otherwise assemblages reflect different bulk compositions and could have equilibrated (but not necessarily) at the same conditions. These two situations are referred to as *incompatible* and *compatible* assemblages, respectively (Fisher, 1990).

Incompatibility reactions correspond to crossing tielines in the relevant compositional space (Fig. 1). These relationships can be investigated by graphical analysis of phase diagrams, such as the AFM projection of Thompson (1957) for the model pelitic system. However, in complex systems such as natural rocks, where extra components (e.g. MnO) may not be negligible, the limitation of plots to two dimensions makes meaningful graphical representation impossible. As pointed out by Greenwood (1967), algebraic analysis can overcome this problem, because linear dependencies between minerals in the whole multicomponent system do represent incompatibilities. Algebraic analysis was generally performed by regression techniques (Fletcher & Greenwood, 1979; Pigage, 1982; Lang & Rice, 1985; Giaramita & Day, 1991) until Fisher (1989) proposed an alternative technique based on singular value decomposition

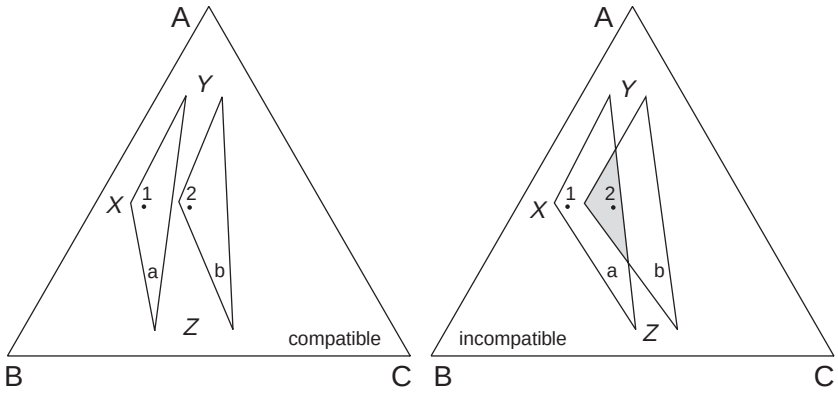

Fig. 1. Graphical description of compatibility relationships between three-phase (X, Y, Z) assemblages (a and b) in a schematic three-component (A–B–C) phase diagram. Compatible assemblages (left) do not intersect, whereas incompatible assemblages (right) have a compositional intersection (shaded), and must be representative of two different mineral facies. All compositions in the shaded area (and only these) can develop both assemblages and thus can belong to both mineral facies.

(SVD). SVD analysis of metamorphic assemblages is becoming increasingly used (Powell, 1990; Gordon *et al*., 1991; Lang, 1991; Hartel & Pattison, 1996).

In this paper, along with discussion of chemical data, the SVD technique is applied to some metapelites from the Vedrette di Ries contact aureole, which contain peculiar nodular textures interpreted as pseudomorphs after a primary garnet. The aim of this study is twofold, looking for incompatibilities among the samples (a) to test the assumption of a common protolith, and (b) if possible, to identify the mass balances or chemical relationships existing within single samples and among sample pairs, comparing them with the inferences provided by the microstructures. It will also be shown that integration between microstructural analysis and mass-balance inspection can lead to a deeper insight into reaction mechanisms, such as ionic reaction cycles.

GEO-PETROGRAPHIC BACKGROUND

Details on the geological setting, location, mineral assemblages and textures of the four metapelites studied in this work (VR491, VR496, VR480 & VR466, hereafter referred as A, B, C & D) can be found in a companion paper (Cesare, 1999) describing the metamorphic evolution of these rocks. The metapelites occur in the aureole of the Vedrette di Ries tonalite, and belong to the Austroalpine basement of the eastern Alps. These rocks were involved in both pre-Alpine and polyphase Alpine metamorphic cycles (Borsi *et al*., 1973); the latter terminated during the Oligocene with emplacement of the Vedrette di Ries pluton (Bellieni *et al*., 1981) and the development of the contact effects that are the main subject of this study. The samples were collected in well-defined layers that crop out at variable distance from the intrusion and belong to different metamorphic zones in the aureole; their mineralogy is listed in Table 1. The contact metamorphic grade increases in samples according to the sequence: A < B < C < D.

Table 1. Mineral assemblages of the four metapelite samples. Fib, fibrolite; Ser, sericite.

	Sample			
	A	B	C	D
And		X	X	X
Bt	X	X	X	X
Chl	X	X	X	
Fib	X	X		X
Grt	X	X	X	
Ilm	X	X	X	X
Ky	X	X		
Ms	X	X	X	X
Pl	X	X	X	X
Qtz	X	X	X	X
Ser	X	X	X	
St	X	X	X	X

Sample A, the most external, was slightly affected by contact metamorphism, and contains abundant relicts (kyanite, garnet and fibrolite) of earlier parageneses, both Alpine and pre-Alpine in age. A small amount of staurolite occurs as overgrowths on kyanite; the latter forms typical microgranular nodules. These nodules, immersed in a sericite-rich matrix, represent pseudomorphs after garnet.

Sample B contains abundant staurolite, both in the nodules and in the matrix, where biotite recrystallizes with random orientation. Andalusite porphyroblasts overgrow the foliation, and are mainly localized in the sericite-rich portions. Because biotite and staurolite inclusions in andalusite are finer than outside andalusite, it is suggested that growth of andalusite and staurolite, and coarsening of biotite-bearing matrix, were synchronous and occurred during contact metamorphism.

Sample C has a similar mineralogy to B, but chlorite and muscovite are less abundant, garnet occurs as scarce relict inclusions, kyanite is lacking, and

staurolite, biotite and andalusite are more abundant and coarser.

Sample D contains nodules of decussate muscovite, where relict inclusions of staurolite from former aggregates are occasionally preserved. Both andalusite and fibrolite are abundant, but the former shows dissolution textures, indicating that it is metastable. The rock matrix is mainly composed of biotite–fibrolite folia alternating with quartz–plagioclase layers. Staurolite does not occur in the matrix, and muscovite is mainly concentrated in the nodules.

Based on the peculiar features of these rocks, Cesare (1999) proposes that nodular textures represent stages in a sequence of pseudomorphs after garnet, and suggests that (i) the four metapelites share a common protolith, possibly (re)folded during polymetamorphism, prior to the emplacement of Vedrette di Ries tonalite, and (ii) that the AFM reactions

$$\mathrm{Ky} + \mathrm{Grt} + \mathrm{Ms} + \mathrm{Chl} = \mathrm{St} + \mathrm{And} + \mathrm{Bt} \qquad (1)$$

and

$$\mathrm{St} + \mathrm{And} + \mathrm{Chl} + \mathrm{Ms} = \mathrm{Bt} + \mathrm{Sil} \qquad (2)$$

could describe the mineralogical changes among samples (A→C and C→D, respectively). In this model, the reactions, as well as the differentiation from the common protolith, are believed to have occurred during the Oligocene contact metamorphism. Reactions (1) and (2) involve a different Al_2SiO_5 polymorph on each side: kyanite is a relict of regional metamorphism, whereas andalusite and fibrolite develop during progressive contact metamorphism. As a consequence, both reactions need also to account for an Al_2SiO_5 phase transition.

MINERAL CHEMISTRY

Chemical analyses of all mineral phases in the metapelites were obtained using a Cameca SX50 electron microprobe at the Institute of Mineralogy and Petrology of the ETH (Zürich), using a beam current of 20 nA and an accelerating voltage of 15 kV. A focused beam of *c.* 1 μm was used for all analyses, although this may have enhanced volatile loss on micas and plagioclase. Natural oxides and silicates were used as standards. Compositions reported in Table 2 are averages of all spot analyses of each phase in a sample. Also reported are single spot analyses of phases which show compositional inhomogeneities, discussed below. Where not specified, the variation of each element in each mineral can be deduced from the standard deviation values (1 σ) in Table 2 and the error matrices of Tables 5–8.

Andalusite and *kyanite* have low Fe contents (<0.02 atoms), that do not affect phase relationships; fibrolite in sample D could not be analysed because of contamination from finely intergrown biotite.

Biotite is very similar (average $X_{Fe} = 0.52$–0.55, $\mathrm{Ti} = 0.17 \pm 0.02$ atoms) in samples A, B and C, with increases in sample D for Ti (0.28 atoms), Mn (0.18 atoms) and X_{Fe} (0.61). Within the same sample, the only significant variation is represented by the changes of X_{Fe} within $\pm 3\%$ of the average value, as a function of the co-existing ferromagnesian phase.

Chlorite is homogeneous in each sample, with similar X_{Fe} in the range 0.49 ± 0.02. Samples B and C, which belong to the same zone (andalusite–staurolite) show, with decreasing distance from the intrusion, higher Mn (like biotite), Si (from 2.56 to 2.64 atoms) and lower Al (from 2.92 to 2.84); this is typical of progressive metamorphism (e.g. Pattison, 1987).

Garnet is the only mineral phase with a well-developed zoning, as can be deduced from the point analyses G1–G5 and the large standard deviations reported in Table 2. The largest variations involve Mn (from 0.04 to 0.32 atoms); in sample B this may also reflect the presence of two garnet generations, the second (with low Mn content) forming either overgrowths on earlier porphyroclasts (analysis G4), or fine-grained rims around biotite in the matrix (analysis G5).

Ilmenite is close to stoichiometry in samples A and B, whereas it contains appreciable Mn (0.05 atoms) in sample D.

Muscovite analyses vary in their Ti content (from 0.01 to 0.09 atoms) and $\mathrm{K}/(\mathrm{K} + \mathrm{Na})$ value (from 0.73 to 0.91). In samples A and B, this reflects the presence of two mica generations: coarse muscovite (analyses M1 & M3) and sericite (analyses M2 & M4), which differ mainly in their Ti content (up to 0.07 atoms in muscovite). Differences in composition also occur in sample D, where decussate muscovite in nodules has lower Ti (0.04 atoms, analysis M5) than muscovite in the matrix (0.09 atoms, analysis M6).

Plagioclase shows a slight increase in anorthite from A ($X_{An} = 0.11$) to D ($X_{An} = 0.18$). Notable plagioclase zoning was not observed, and in each sample the anorthite variation is restricted within ± 0.03.

Staurolite does not show appreciable variations of X_{Fe} (0.84 to 0.87) with metamorphic grade, whereas an increase of Mn (from 0.02–0.11 atoms) is observed. Staurolite has low Zn content in all samples except D, where up to 0.30 atoms are present, corresponding to a $\mathrm{Zn}/(\mathrm{Zn} + \mathrm{Fe} + \mathrm{Mg} + \mathrm{Mn})$ ratio of 0.07. The Zn concentration is in negative correlation with the modal abundance of staurolite in the samples, as pointed out by Guidotti (1970). Owing to the incompleteness of information on all minerals (see discussion in Tuisku *et al*., 1987), the Zn component could not be considered in the matrix analysis.

Mineral compositions suggest that, with the exception of garnet in sample B and to a lesser extent of muscovite in samples A, B and D, the four samples may represent a good approach to equilibrium and can then be modelled by the SVD technique.

BULK CHEMISTRY

Whole rock XRF & AA data of the four metapelites are reported in Table 3. The greatest variation among samples involves SiO_2 (49.62–61.15 wt%), which in turn affects all the other oxides. Such changes are probably related to local variations in the abundance of quartz layers within the samples. This hypothesis has been tested by normalizing bulk compositions on a silica-free, anhydrous basis: i.e. by projecting from quartz and H_2O, as on the AFM diagram. As shown by the data in Table 4 and in particular by the values of Al_2O_3, the variations of oxides after normalization are much smaller than suggested by Table 3, generally within 10% relative.

In the AFM diagram of Fig. 2(a), bulk compositions project within a very restricted area within the intersection of all fields defined by each sample assemblage. Although assemblages comprise phases that are in clear disequilibrium (e.g. kyanite in A and B, or andalusite in D), these phases have to be included in order to account for the full chemistry of the system. Garnet and staurolite, respectively included in assemblages C and D, occur in negligible amount: omission of these phases would greatly decrease the intersection volume of assemblages, but still all bulk compositions would plot inside it (Fig. 2b).

MATRIX ANALYSIS: SVD METHOD AND INPUT DATA

Linear dependencies between minerals in a single sample assemblage represent crossing tie-lines in an appropriate phase diagram; these relationships have several interpretations (Fisher, 1989), such as disequilibrium in the assemblage, or equilibration under imposed external conditions. They may also indicate the process by which the assemblage developed, for example, an univariant reaction. It is

Table 2. Microprobe analyses of mineral phases in the four metapelite samples, generally expressed as average and standard deviation of *n* data points. Also reported are point analyses of garnet and muscovite (labelled Gx and Mx, respectively), where significant inhomogeneities have been detected.

$X_{Fe} = Fe/(Fe+Mg)$, $X_{Alm} = Fe/(Fe+Mg+Mn+Ca)$; $X_{Pyp} = Mg/(Fe+Mg+Mn+Ca)$; $X_{Sps} = Mn/(Fe+Mg+Mn+Ca)$; $X_{Grs} = Ca/(Fe+Mg+Mn+Ca)$; $X_{Ms} = K/(Na+K)$; $X_{An} = Ca/(Na+Ca)$.

Aluminium silicates (5 oxygen)

	A (Ky) $n=1$	B (And) $n=4$ (1 σ)	C (And) $n=13$ (1 σ)	D (And) $n=5$ (1 σ)
SiO_2	37.85	36.82 (0.38)	36.85 (0.17)	36.71 (0.53)
TiO_2	0.00	0.05 (0.04)	0.03 (0.02)	0.03 (0.03)
Al_2O_3	63.18	62.93 (0.62)	62.98 (0.22)	62.92 (0.48)
Fe_2O_3	0.35	0.66 (0.24)	0.37 (0.12)	0.32 (0.05)
MnO	0.00	0.00 (0.01)	0.01 (0.01)	0.00 (0.00)
MgO	0.01	0.10 (0.04)	0.05 (0.01)	0.04 (0.02)
CaO	0.00	0.01 (0.01)	0.01 (0.01)	0.00 (0.00)
Na_2O	0.00	0.01 (0.01)	0.01 (0.01)	0.01 (0.01)
K_2O	0.00	0.00 (0.01)	0.00 (0.01)	0.01 (0.01)
Total	101.39	100.58 (0.51)	100.31 (0.27)	100.05 (0.92)
Si	1.01	0.99 (0.01)	0.99 (0.00)	0.99 (0.01)
Ti	0.00	0.00 (0.00)	0.00 (0.00)	0.00 (0.00)
Al	1.98	2.00 (0.01)	2.00 (0.01)	2.00 (0.01)
Fe^{3+}	0.01	0.01 (0.01)	0.01 (0.00)	0.01 (0.00)
Mn	0.00	0.00 (0.00)	0.00 (0.00)	0.00 (0.00)
Mg	0.00	0.00 (0.00)	0.00 (0.00)	0.00 (0.00)
Ca	0.00	0.00 (0.00)	0.00 (0.00)	0.00 (0.00)
Na	0.00	0.00 (0.00)	0.00 (0.00)	0.00 (0.00)
K	0.00	0.00 (0.00)	0.00 (0.00)	0.00 (0.00)

Biotite (22 oxygen, anhydrous)

	A $n=19$ (1 σ)	B $n=20$ (1 σ)	C $n=53$ (1 σ)	D $n=4$ (1 σ)
SiO_2	35.79 (0.43)	35.45 (0.39)	35.92 (0.49)	34.36 (0.53)
TiO_2	1.40 (0.10)	1.48 (0.09)	1.48 (0.15)	2.38 (0.4)
Al_2O_3	19.57 (1.06)	19.62 (0.30)	19.58 (0.52)	19.79 (0.42)
FeO	18.82 (0.96)	19.66 (0.54)	19.66 (0.92)	21.12 (0.46)
MnO	0.02 (0.02)	0.05 (0.03)	0.08 (0.03)	0.18 (0.03)
MgO	9.40 (0.50)	9.66 (0.26)	9.43 (0.35)	7.61 (0.32)
CaO	0.00 (0.01)	0.01 (0.01)	0.01 (0.01)	0.01 (0.01)
Na_2O	0.22 (0.08)	0.28 (0.08)	0.40 (0.11)	0.22 (0.09)
K_2O	9.45 (0.31)	8.69 (0.18)	8.68 (0.20)	8.85 (0.27)
Total	94.68 (0.48)	94.89 (0.35)	95.25 (0.63)	94.51 (0.56)
Si	5.46 (0.04)	5.40 (0.04)	5.44 (0.04)	5.31 (0.06)
Ti	0.16 (0.01)	0.17 (0.01)	0.17 (0.02)	0.28 (0.05)
Al	3.52 (0.16)	3.52 (0.05)	3.50 (0.08)	3.61 (0.07)
Fe^{2+}	2.40 (0.14)	2.50 (0.07)	2.49 (0.13)	2.73 (0.07)
Mn	0.00 (0.00)	0.01 (0.00)	0.01 (0.00)	0.02 (0.00)
Mg	2.14 (0.12)	2.19 (0.06)	2.13 (0.08)	1.75 (0.07)
Ca	0.00 (0.00)	0.00 (0.00)	0.00 (0.00)	0.00 (0.00)
Na	0.07 (0.02)	0.08 (0.02)	0.12 (0.03)	0.06 (0.03)
K	1.84 (0.05)	1.69 (0.04)	1.68 (0.04)	1.75 (0.04)
X_{Fe}	0.53 (0.01)	0.53 (0.01)	0.54 (0.01)	0.61 (0.01)

Chlorite (10 oxygen, anhydrous)

	A $n=3$ (1 σ)	B $n=13$ (1 σ)	C $n=9$ (1 σ)
SiO_2	24.16 (0.36)	24.27 (0.33)	25.09 (0.34)
TiO_2	0.12 (0.03)	0.10 (0.02)	0.08 (0.03)
Al_2O_3	22.89 (0.33)	23.49 (0.36)	22.95 (0.56)
FeO	25.21 (0.28)	25.25 (0.18)	24.81 (0.53)
MnO	0.03 (0.03)	0.07 (0.02)	0.17 (0.02)
MgO	14.08 (0.35)	14.46 (0.34)	14.34 (0.64)
CaO	0.01 (0.01)	0.01 (0.01)	0.01 (0.01)
Na_2O	0.00 (0.00)	0.01 (0.01)	0.01 (0.02)
K_2O	0.02 (0.01)	0.02 (0.02)	0.02 (0.02)
Total	86.53 (0.48)	87.69 (0.53)	87.47 (0.65)
Si	2.58 (0.02)	2.56 (0.02)	2.64 (0.02)
Ti	0.01 (0.00)	0.01 (0.00)	0.01 (0.00)
Al	2.88 (0.04)	2.92 (0.03)	2.84 (0.06)
Fe^{2+}	2.25 (0.03)	2.22 (0.02)	2.18 (0.04)
Mn	0.00 (0.00)	0.01 (0.00)	0.02 (0.00)
Mg	2.24 (0.05)	2.27 (0.06)	2.25 (0.11)
Ca	0.00 (0.00)	0.00 (0.00)	0.00 (0.00)
Na	0.00 (0.00)	0.00 (0.00)	0.00 (0.00)
K	0.00 (0.00)	0.00 (0.00)	0.00 (0.00)
X_{Fe}	0.50 (0.01)	0.50 (0.01)	0.49 (0.02)

Garnet (12 oxygen)

	A			B				C
	G1 Core	G2 Rim	$n=15$ (1 σ)	G3 Core	G4 Rim	G5 Rim on Bt	$n=70$ (1 σ)	$n=13$ (1 σ)
SiO_2	37.25	37.53	37.53 (0.27)	36.79	36.17	36.84	37.09 (0.25)	37.14 (0.18)
Al_2O_3	20.82	21.41	21.10 (0.19)	21.18	24.32	21.26	21.18 (0.43)	20.95 (0.16)
FeO	37.55	36.03	37.17 (0.48)	34.45	34.09	37.25	35.17 (1.44)	33.08 (0.63)
MnO	1.53	0.52	1.11 (0.42)	4.67	2.62	1.37	3.72 (1.87)	4.45 (0.14)
MgO	2.74	4.01	3.08 (0.53)	2.93	2.33	2.72	2.71 (0.34)	2.18 (0.09)
CaO	0.55	0.61	0.69 (0.18)	0.63	0.65	1.18	0.75 (0.33)	2.02 (0.47)
Total	100.44	100.12	100.67 (0.41)	100.65	100.19	100.61	100.62 (0.45)	99.82 (0.58)
Si	3.00	3.00	3.01 (0.01)	2.97	2.89	2.97	2.98 (0.02)	3.01 (0.01)
Al	1.98	2.02	1.99 (0.01)	2.01	2.29	2.02	2.01 (0.04)	2.00 (0.02)
Fe^{2+}	2.53	2.41	2.49 (0.04)	2.32	2.28	2.51	2.37 (0.09)	2.24 (0.04)
Mn	0.10	0.04	0.08 (0.03)	0.32	0.18	0.09	0.25 (0.13)	0.31 (0.01)
Mg	0.33	0.48	0.37 (0.06)	0.35	0.28	0.33	0.32 (0.04)	0.26 (0.01)
Ca	0.05	0.05	0.06 (0.02)	0.05	0.06	0.10	0.06 (0.03)	0.18 (0.04)
X_{Alm}	0.84	0.81	0.83 (0.01)	0.76	0.82	0.83	0.79 (0.03)	0.75 (0.01)
X_{Pyp}	0.11	0.16	0.12 (0.02)	0.12	0.10	0.11	0.11 (0.01)	0.09 (0.00)
X_{Sps}	0.03	0.01	0.03 (0.01)	0.10	0.06	0.03	0.08 (0.04)	0.10 (0.00)
X_{Grs}	0.02	0.02	0.02 (0.01)	0.02	0.02	0.03	0.02 (0.01)	0.06 (0.01)
X_{Fe}	0.88	0.83	0.87 (0.02)	0.87	0.89	0.88	0.88 (0.01)	0.89 (0.00)

Ilmenite (3 oxygen, 2 cations)

	A $n=2$ (1 σ)	B $n=1$	D $n=1$
TiO_2	52.07 (1.02)	53.19	52.94
Al_2O_3	0.09 (0.13)	0.00	0.15
FeO	45.34 (0.09)	45.99	42.66
MnO	0.52 (0.13)	0.52	2.29
MgO	0.05 (0.01)	0.03	0.04
Total	98.07 (0.84)	99.73	98.08
Ti	1.00 (0.02)	1.01	1.02
Al	0.00 (0.00)	0.00	0.00
Fe^{2+}	0.97 (0.00)	0.97	0.92
Mn	0.01 (0.01)	0.01	0.05
Mg	0.00 (0.00)	0.00	0.00

Muscovite (22 oxygen, anhydrous)

	A			B			C	D		
	M1 Coarse	M2 Sericite	$n=3$ (1 σ)	M3 Coarse	M4 Sericite	$n=13$ (1 σ)	$n=7$ (1 σ)	M5 Nodule	M6 Matrix	$n=7$ (1 σ)
SiO_2	46.06	47.13	46.20 (0.54)	45.66	47.13	45.97 (0.89)	46.04 (0.45)	45.55	46.07	45.51 (0.38)
TiO_2	0.73	0.10	0.54 (0.33)	0.69	0.10	0.58 (0.20)	0.28 (0.12)	0.37	0.88	0.47 (0.32)
Al_2O_3	36.01	35.44	35.95 (0.50)	37.04	35.44	36.96 (0.73)	36.79 (0.37)	37.52	37.24	37.38 (0.24)
FeO	1.56	1.14	1.28 (0.40)	1.32	1.14	1.14 (0.18)	0.90 (0.13)	0.92	1.11	0.92 (0.11)
MnO	0.03	0.00	0.02 (0.02)	0.01	0.00	0.01 (0.01)	0.01 (0.01)	0.02	0.00	0.01 (0.01)
MgO	0.58	1.21	0.59 (0.02)	0.57	1.21	0.59 (0.23)	0.50 (0.08)	0.52	0.44	0.46 (0.07)
CaO	0.00	0.01	0.00 (0.00)	0.01	0.01	0.01 (0.01)	0.01 (0.03)	0.01	0.01	0.01 (0.01)
Na_2O	1.01	1.39	1.25 (0.28)	1.18	1.39	1.55 (0.34)	1.61 (0.09)	1.01	0.95	0.86 (0.28)
K_2O	10.08	8.44	9.42 (0.71)	9.26	8.44	8.55 (0.51)	8.19 (0.38)	8.78	9.12	8.98 (0.43)
Total	96.07	94.86	95.24 (0.74)	95.74	94.86	95.36 (0.75)	94.33 (0.88)	94.69	95.84	94.60 (0.66)
Si	6.09	6.23	6.13 (0.04)	6.02	6.23	6.06 (0.09)	6.11 (0.03)	6.03	6.05	6.04 (0.02)
Ti	0.07	0.01	0.05 (0.03)	0.07	0.01	0.06 (0.02)	0.03 (0.01)	0.04	0.09	0.05 (0.03)
Al	5.61	5.52	5.62 (0.04)	5.76	5.52	5.74 (0.12)	5.75 (0.06)	5.86	5.76	5.85 (0.06)
Fe^{2+}	0.17	0.13	0.14 (0.04)	0.15	0.13	0.13 (0.02)	0.10 (0.01)	0.10	0.12	0.10 (0.01)
Mn	0.00	0.00	0.00 (0.00)	0.00	0.00	0.00 (0.00)	0.00 (0.00)	0.00	0.00	0.00 (0.00)
Mg	0.12	0.24	0.12 (0.01)	0.11	0.24	0.12 (0.04)	0.10 (0.02)	0.10	0.09	0.09 (0.01)
Ca	0.00	0.00	– (0.00)	0.00	0.00	0.00 (0.00)	0.00 (0.00)	0.00	0.00	0.00 (0.00)
Na	0.26	0.36	0.32 (0.07)	0.30	0.36	0.40 (0.09)	0.41 (0.02)	0.26	0.24	0.22 (0.07)
K	1.70	1.42	1.59 (0.12)	1.56	1.42	1.44 (0.09)	1.39 (0.06)	1.48	1.53	1.52 (0.07)
X_{Ms}	0.87	0.80	0.83 (0.04)	0.84	0.80	0.78 (0.05)	0.77 (0.01)	0.85	0.86	0.87 (0.04)

Plagioclase (8 oxygen)

	A $n=6$ (1 σ)	B $n=3$ (1 σ)	C $n=5$ (1 σ)	D $n=4$ (1 σ)
SiO_2	66.27 (0.69)	64.94 (0.35)	64.89 (0.63)	63.27 (0.56)
Al_2O_3	21.63 (0.41)	22.49 (0.03)	22.27 (0.35)	23.12 (0.97)
CaO	2.28 (0.41)	3.01 (0.18)	2.99 (0.30)	3.54 (0.46)
Na_2O	10.31 (0.33)	9.57 (0.06)	9.52 (0.17)	8.91 (0.66)
K_2O	0.07 (0.02)	0.05 (0.01)	0.10 (0.02)	0.08 (0.03)
Total	100.55 (0.51)	100.06 (0.61)	99.77 (0.34)	98.92 (0.33)
Si	2.89 (0.02)	2.87 (0.00)	2.87 (0.02)	2.83 (0.02)
Al	1.11 (0.02)	1.17 (0.01)	1.16 (0.02)	1.22 (0.05)
Ca	0.11 (0.02)	0.14 (0.01)	0.14 (0.01)	0.17 (0.02)
Na	0.87 (0.02)	0.82 (0.00)	0.82 (0.02)	0.77 (0.06)
K	0.00 (0.00)	0.00 (0.00)	0.01 (0.00)	0.01 (0.00)
X_{An}	0.11 (0.02)	0.15 (0.01)	0.15 (0.01)	0.18 (0.03)

Staurolite (48 oxygen, anhydrous)

	A $n=10$ (1 σ)	B $n=45$ (1 σ)	C $n=97$ (1 σ)	D $n=10$ (1 σ)
SiO_2	28.52 (0.18)	27.83 (0.29)	27.83 (0.33)	28.07 (0.48)
TiO_2	0.51 (0.07)	0.54 (0.11)	0.47 (0.11)	0.50 (0.17)
Al_2O_3	54.45 (0.27)	54.49 (0.33)	54.79 (0.42)	54.78 (0.39)
FeO	12.68 (0.26)	13.46 (0.46)	13.09 (0.44)	11.86 (0.40)
MnO	0.09 (0.02)	0.12 (0.02)	0.26 (0.04)	0.46 (0.06)
MgO	1.05 (0.12)	1.46 (0.20)	1.35 (0.19)	1.02 (0.11)
ZnO	0.26 (0.06)	0.20 (0.08)	0.12 (0.07)	1.26 (0.21)
CaO	0.01 (0.01)	0.01 (0.01)	0.00 (0.01)	0.00 (0.00)
Na_2O	0.02 (0.01)	0.01 (0.01)	0.01 (0.01)	0.02 (0.03)
K_2O	0.01 (0.02)	0.01 (0.01)	0.01 (0.01)	0.00 (0.01)
Total	97.60 (0.60)	98.13 (0.30)	97.94 (0.27)	97.98 (0.29)
Si	7.79 (0.05)	7.60 (0.08)	7.60 (0.09)	7.67 (0.13)
Ti	0.11 (0.02)	0.11 (0.02)	0.10 (0.02)	0.10 (0.04)
Al	17.83 (0.09)	17.84 (0.11)	17.94 (0.14)	17.93 (0.13)
Fe^{2+}	2.95 (0.06)	3.13 (0.11)	3.04 (0.10)	2.76 (0.09)
Mn	0.02 (0.00)	0.03 (0.01)	0.06 (0.01)	0.11 (0.01)
Mg	0.44 (0.05)	0.61 (0.08)	0.56 (0.08)	0.42 (0.05)
Zn	0.05 (0.01)	0.04 (0.02)	0.03 (0.01)	0.26 (0.04)
Ca	0.00 (0.00)	0.00 (0.00)	0.00 (0.00)	0.00 (0.00)
Na	0.01 (0.01)	0.01 (0.01)	0.01 (0.00)	0.01 (0.01)
K	0.01 (0.01)	0.00 (0.00)	0.00 (0.00)	0.00 (0.00)
X_{Fe}	0.87 (0.01)	0.84 (0.02)	0.85 (0.02)	0.87 (0.01)

Table 3. Bulk rock compositions of the four metapelite samples.

	Sample			
	A	B	C	D
SiO_2	61.15	61.03	49.62	55.86
TiO_2	0.96	0.82	1.32	1.22
Al_2O_3	19.94	18.63	26.53	23.34
FeO_{Total}	7.39	7.46	8.88	8.67
MnO	0.09	0.09	0.09	0.08
MgO	2.23	2.32	2.79	2.71
CaO	0.38	0.39	0.68	0.49
Na_2O	0.77	1.12	1.31	0.45
K_2O	3.92	3.37	4.71	3.82
P_2O_5	0.17	0.15	0.24	0.24
L.O.I.	2.37	3.02	3.23	2.79
Total	99.37	98.40	99.40	99.67

Table 4. Silica-free, anhydrous bulk compositions of metapelite samples, re-cast to an arbitrary total of 45.00.

	Sample			
	A	B	C	D
TiO_2	1.21	1.07	1.28	1.34
Al_2O_3	25.03	24.41	25.65	25.60
FeO_{Total}	9.28	9.77	8.58	9.51
MnO	0.11	0.12	0.09	0.09
MgO	2.80	3.04	2.70	2.97
CaO	0.48	0.51	0.66	0.54
Na_2O	0.97	1.47	1.27	0.49
K_2O	4.92	4.41	4.55	4.19
P_2O_5	0.21	0.20	0.23	0.26
Total	45.00	45.00	45.00	45.00

the aim of the first part of SVD analysis, where single matrices are explored, to constrain the reactions leading to assemblage development by integration with careful textural and field information. In the second part, matrix analysis is applied to pairs of assemblages, because the existence of mass balances implies different equilibration conditions that could be reflected by changes in the topology of phase diagrams.

SVD-based matrix analysis of mineral assemblages was performed with version 2.0 of the programs (CALCWT, MULTI, SVDMOD) written and described by Fisher (1989). For each sample, two input matrices, the composition and the error matrices, were first formed (Tables 5–8). Each matrix contains a number of columns equal to the number of mineral phases in the assemblage (as in Table 1) and eight rows corresponding to the analysed chemical components (Ti, Al, Fe^{2+}, Mn, Mg, Ca, Na, K). The composition matrix contains the averaged analyses, as cations per unit formula (see Table 2); formulae of hydrous phases were calculated on an anhydrous basis, assuming that an H_2O-bearing fluid phase was present during metamorphism to allow for H_2O balancing; Fe was considered to be Fe^{2+} in all minerals. In the matrices, the Si component row was omitted, as well as the quartz phase column, as a means of facilitating computation of rank. This omission is legal (Fisher, 1989) because quartz is in excess in all assemblages. Ilmenite is present but could not be analysed in sample C, where it was assumed to have the same composition as in sample D. Other assumptions involve the Al_2SiO_5 polymorphs, two of which occur in the same sample: fibrolite and kyanite in A, kyanite and andalusite in B, andalusite and fibrolite in D. Because these phases are virtually identical in composition, one can be omitted in each matrix. This does not affect the results of matrix analysis, because SVD programs can handle Al_2SiO_5 compositions as both reactant or product, and because the role of each polymorph was constrained by field and textural analysis. The only restriction of this approach is that the transitions Ky→And and An→Sil cannot be investigated: these have

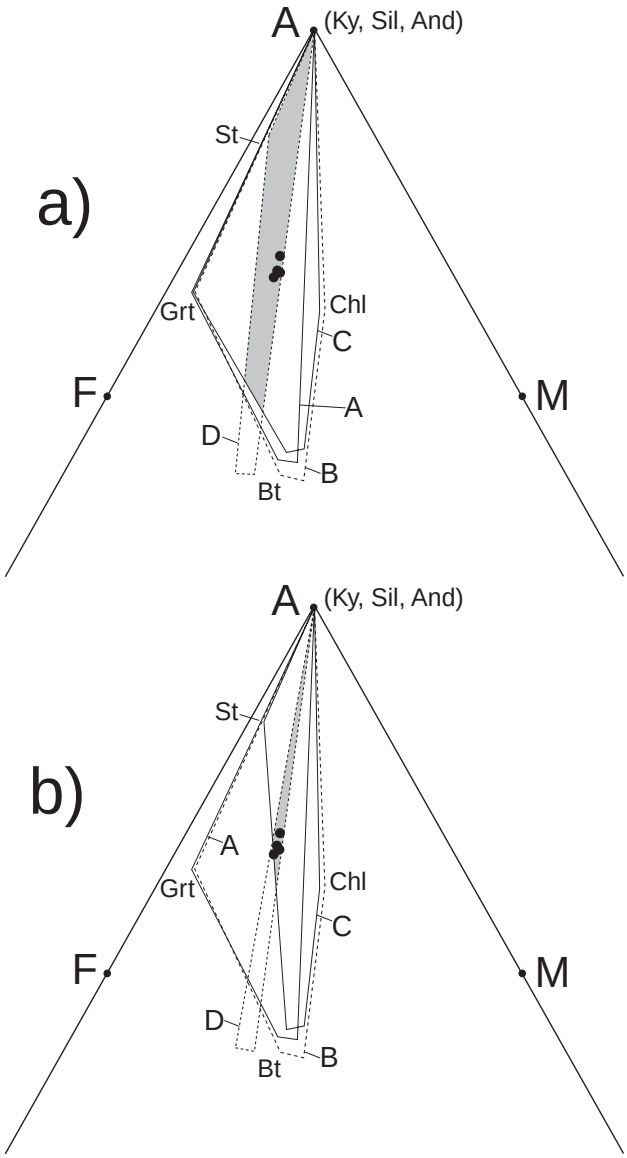

Fig. 2. (a) AFM phase diagram representing the four sample assemblages, drawn on the basis of average measured phase compositions, as in Table 2. Dots represent projected bulk compositions of samples, as in Table 3. The shaded field is the intersection of all sample assemblages. (b) Same as (a), excluding garnet from sample C and staurolite from sample D.

to be considered separately and added to the possible results of matrix analysis.

The error matrices contain the 1 σ standard deviations of the averages reported in each composition matrix; in addition to analytical uncertainties, errors account also for chemical variations between and within grains. In the error matrices, when only one analysis was available for a phase so that the standard deviation was not available (e.g. $ilmenite_D$, $plagioclase_A$), the error has been set to a value of 0.004 as suggested by the SVDMOD program. The same error of 0.004 has been attributed in the case of the element not analysed (e.g. Na in garnet, see Table 2); this procedure avoids a zero divide in the calculations. A few high errors are present: Mn in garnet is due to the chemical zoning, like Ca and Na in plagioclase from sample D; Mg in staurolite and K and Na in muscovite are due to both chemical dishomogeneities within the specimen and

analytical problems such as Na loss. As a whole, error values are similar to those used in the analyses of Lang & Rice (1985), Lang (1991) or Giaramita & Day (1991).

MATRIX ANALYSIS: SVD RESULTS

Sample A

After omission of Si and quartz, the 8×8 matrix A (Table 5) contains Ti, Al, Fe, Mn, Mg, Ca, Na and K as rows, and ilmenite, staurolite, kyanite, biotite, chlorite, garnet, plagioclase and muscovite as columns. The phase rule indicates that if the number of independent compositional parameters is identical to the number of analysed components, then the equilibrium of the eight phases is divariant. To verify that each component imposes an additional dimension, the matrix rank was reduced and a new model matrix of rank 7 was obtained. Matrix rank can be reduced to any value lower than the initial, but the adequacy of the resulting model to represent the initial composition matrix has to be evaluated. The SVDMOD program does this by calculating first the residuals between the model and the analytical compositions, and then the error ratios between the residuals and the uncertainties of the error matrix. These ratios provide an estimate of the adequacy of the fit: as outlined by Fisher (1989) the model matrix is adequate when at least 95% of them are <1 and none is much larger than 2. In the rank 7 model matrix of sample A, all the error ratios are <2.1, and only three (all relevant to the Ca component) are >1; thus, the model represents an adequate fit to the initial matrix. Rank reduction to six leads to a model with seven error ratios >1, three of which are >3; this model was not considered acceptable.

The rank 7 model defines the mass balance:

$$5.000\ \mathrm{Ky} + 0.269\ \mathrm{Grt} + 0.965\ \mathrm{Bt} + 0.314\ \mathrm{Pl} = 0.049\ \mathrm{Ilm} + 1.115\ \mathrm{Ms} + 0.849\ \mathrm{Chl} + 0.306\ \mathrm{St} \quad (3)$$

This linear dependency among minerals is equivalent to a tie-line intersection (i.e. a univariant eight-phase assemblage in a seven-component system), and indicates that the assemblage cannot have equilibrated at arbitrary external conditions. This relation also suggests that the early stage of staurolite growth during contact metamorphism, observed in this sample, occurred by consumption of kyanite, biotite and garnet, and production of muscovite and chlorite; this is in agreement with the textural observations of Cesare (1999).

Sample B

The 8×8 matrix B (Table 6) contains ilmenite, staurolite, Al_2SiO_5 (kyanite or andalusite), biotite, chlorite, garnet, plagioclase and muscovite; it has rank eight and does not contain any mass balance. The matrix of reduced rank (7) contains six error ratios >1, two of which much larger than two (7.4 & 5.9); it must be considered a first-order model of the compositional matrix. This model defines the mass balance

$$0.133\ \mathrm{Ilm} + 0.100\ \mathrm{St} + 1.329\ \mathrm{Chl} + 1.768\ \mathrm{Ms} + 0.107\ \mathrm{Grt} = 5.000\ \mathrm{Al_2SiO_5} + 1.511\mathrm{Bt} + 0.631\ \mathrm{Pl} \quad (4)$$

which would suggest an expanded form of the AFM reaction $\mathrm{St} + \mathrm{Chl} = \mathrm{Bt} + \mathrm{And}$. Note that the stoichiometric coefficient for staurolite is low, such that staurolite contributes <10 wt% of the total Al and Fe involved in the mass balance.

Large residuals and error ratios are related to the high Mn (0.25) of averaged garnet composition used in the input matrix; in fact, if low-Mn garnet rim (analysis G5 in Table 2) is used in the input matrix, the modified rank 7 model is acceptable as it gives only three error ratios >1 (5.9, 1.8 & 1.1). This suggests that the high Mn cores of garnet porphyroclasts are not in equilibrium with the assemblage, whereas their rims and the small crystals around biotite may be stable during the contact metamor-

Table 5. Input data and errors for single matrix A.

	Ilm	St	Ky	Bt	Chl	Grt	Pl	Ms
Ti	1.004	0.107	0.000	0.160	0.008	0.000	0.000	0.054
Al	0.003	17.826	1.982	3.520	2.902	1.991	1.106	5.616
Fe	0.972	2.946	0.007	2.400	2.267	2.490	0.000	0.142
Mn	0.011	0.022	0.000	0.000	0.004	0.075	0.000	0.002
Mg	0.002	0.436	0.001	2.140	2.223	0.367	0.000	0.117
Ca	0.000	0.002	0.000	0.000	0.002	0.059	0.095	0.000
Na	0.000	0.010	0.000	0.070	0.000	0.000	0.867	0.322
K	0.000	0.005	0.000	1.840	0.001	0.000	0.003	1.592
Errors								
Ti	0.020	0.016	0.004	0.010	0.001	0.004	0.004	0.033
Al	0.004	0.089	0.004	0.160	0.039	0.013	0.023	0.039
Fe	0.004	0.061	0.004	0.140	0.020	0.042	0.004	0.044
Mn	0.014	0.005	0.004	0.001	0.002	0.029	0.004	0.002
Mg	0.004	0.049	0.004	0.120	0.055	0.061	0.004	0.005
Ca	0.004	0.002	0.004	0.001	0.001	0.015	0.019	0.001
Na	0.004	0.008	0.004	0.020	0.001	0.004	0.025	0.071
K	0.004	0.008	0.004	0.050	0.001	0.004	0.001	0.122

Table 6. Input data and errors for single matrix B.

	Ilm	St	Ky/And	Bt	Chl	Grt	Pl	Ms
Ti	1.012	0.113	0.001	0.170	0.008	0.000	0.000	0.057
Al	0.000	17.840	1.995	3.520	2.915	2.009	1.170	5.740
Fe	0.974	3.127	0.013	2.500	2.223	2.367	0.000	0.126
Mn	0.010	0.028	0.000	0.010	0.006	0.253	0.000	0.001
Mg	0.000	0.606	0.004	2.190	2.268	0.325	0.000	0.117
Ca	0.000	0.002	0.000	0.000	0.001	0.065	0.142	0.001
Na	0.000	0.006	0.000	0.080	0.001	0.000	0.819	0.395
K	0.000	0.003	0.000	1.690	0.003	0.000	0.003	1.438
Errors								
Ti	0.004	0.023	0.001	0.010	0.002	0.004	0.004	0.019
Al	0.004	0.109	0.013	0.050	0.034	0.036	0.006	0.118
Fe	0.004	0.107	0.005	0.070	0.020	0.094	0.004	0.021
Mn	0.004	0.005	0.004	0.004	0.002	0.128	0.004	0.001
Mg	0.004	0.084	0.002	0.060	0.057	0.040	0.004	0.044
Ca	0.004	0.002	0.004	0.004	0.001	0.029	0.007	0.001
Na	0.004	0.006	0.004	0.020	0.002	0.004	0.001	0.085
K	0.004	0.003	0.004	0.040	0.002	0.004	0.001	0.087

phism. The modified model matrix defines the mass balance

$$0.301\ \mathrm{Ilm} + 5.000\ \mathrm{Al_2SiO_5} + 1.749\ \mathrm{Chl} + 2.138\mathrm{Ms} + 1.750\ \mathrm{Grt} = 1.313\ \mathrm{St} + 1.828\mathrm{Bt} + 0.857\ \mathrm{Pl} \quad (5)$$

Compared with mass balance (4), this has larger coefficients for all phases, and contains Al_2SiO_5 and staurolite in a reversed position. As staurolite and biotite occur on one side, it can be interpreted as the reaction forming staurolite in sample B. Because it is demonstrated that staurolite grows replacing kyanite, the Al_2SiO_5 in (5) should be interpreted as kyanite. It is apparent that modelling this sample is problematic, since two Al_2SiO_5 polymorphs occur: because of the textural indication that kyanite is a disequilibrium relict, any possible mass balance resulting from matrix analysis must be coupled with the Ky→And transition.

Sample C

The 8×8 matrix C (Table 7) contains ilmenite, staurolite, andalusite, biotite, chlorite, plagioclase, muscovite and garnet; the latter was included in the matrix even if it is present in relict crystals. This matrix does not contain any mass balance, and rank reduction leads to a rank 7 model with six error ratios >1, one of which is >2 (5.4). As they exceed 5% of the total, the model is not fully adequate to represent the composition matrix, and the mass balance that it defines

$$0.142\ \mathrm{Ilmp} + 0.175\ \mathrm{St} + 1.089\ \mathrm{Chl} + 1.533\mathrm{Ms} + 0.003\ \mathrm{Grt} = 5.000\ \mathrm{And} + 1.266\mathrm{Bt} + 0.551\ \mathrm{Pl} \quad (6)$$

must be evaluated with caution. High error ratios are restricted to the Ca and Mn rows, and may indicate that reported concentrations and errors are not fully representative of the chemical system. Because Ca and Mn mostly occur in plagioclase and garnet, this inadequacy may be related to a poor knowledge and description of zoning in these minerals. However, as noted by Hartel & Pattison (1996), another explanation is that plagioclase and garnet compositions may exhibit continuous variations during reactions that cannot be accounted for when only one composition is used in the matrix. Mass balance (6) is very similar to (4) in sample B, but has a much lower coefficient for garnet; it may indicate the progress of an andalusite-forming reaction where garnet is essentially refractory. Although (4) and (6) are the result of questionable models, it will be shown below that these balances are indeed relevant to the interpretation of assemblages.

Sample D

The 8×6 matrix D (Table 8) contains ilmenite, staurolite, Al_2SiO_5 (relict andalusite and sillimanite), biotite, plagioclase and muscovite. Staurolite, present in the rock as rare inclusions in muscovite, is included in the input data as it may represent a nearly exhausted reactant. The initial matrix has rank 6 and does not contain mass balances; rank reduction to 5 defines a model that is not acceptable because it contains very high error ratios. As the system is defined by at least six independent components, the six-phase assemblage in sample D is at least divariant.

Composite matrix A–B

One of the problems of composite matrices is that similar phases (e.g. Ms) are included twice, one for each assemblage, producing incompatibilities with large coefficients of opposite sign for a particular phase and low coefficients for the others in a way such that the general result is, for example, $Bt_A = Bt_B$. Although these relations have a poor significance, the choice was made not to omit phases except for ilmenite and Al_2SiO_5, which have been considered only once in each composite: when searching for incompatibilities, the MULTI program allows them to be computed either as reactants or products.

Table 7. Input data and errors for single matrix C

	Ilm	St	And	Bt	Chl	Pl	Ms	Grt
Ti	1.025	0.099	0.001	0.170	0.006	0.000	0.028	0.000
Al	0.000	17.936	2.000	3.500	2.843	1.162	5.752	1.998
Fe	0.918	3.041	0.008	2.490	2.182	0.000	0.100	2.239
Mn	0.050	0.062	0.000	0.010	0.015	0.000	0.001	0.305
Mg	0.002	0.559	0.002	2.130	2.247	0.000	0.099	0.263
Ca	0.000	0.001	0.000	0.000	0.001	0.142	0.002	0.175
Na	0.000	0.005	0.000	0.120	0.002	0.817	0.414	0.000
K	0.000	0.003	0.000	1.680	0.003	0.005	1.386	0.000
Errors								
Ti	0.004	0.023	0.004	0.020	0.003	0.004	0.012	0.004
Al	0.004	0.137	0.006	0.080	0.059	0.018	0.058	0.016
Fe	0.004	0.102	0.002	0.130	0.042	0.004	0.014	0.039
Mn	0.004	0.008	0.004	0.004	0.002	0.004	0.001	0.010
Mg	0.004	0.077	0.004	0.080	0.108	0.004	0.016	0.011
Ca	0.004	0.002	0.004	0.004	0.001	0.014	0.004	0.040
Na	0.004	0.005	0.004	0.030	0.003	0.015	0.022	0.004
K	0.004	0.004	0.004	0.040	0.003	0.001	0.062	0.004

Table 8. Input data and errors for single matrix D.

	Ilm	St	Al_2SiO_5	Bt	Pl	Ms
Ti	1.025	0.105	0.001	0.280	0.000	0.046
Al	0.000	17.934	2.003	3.610	1.219	5.845
Fe	0.918	2.755	0.007	2.730	0.000	0.102
Mn	0.050	0.109	0.000	0.020	0.000	0.001
Mg	0.002	0.421	0.002	1.750	0.000	0.091
Ca	0.000	0.001	0.000	0.000	0.170	0.001
Na	0.000	0.012	0.001	0.060	0.773	0.220
K	0.000	0.001	0.000	1.750	0.005	1.520
Errors						
Ti	0.004	0.035	0.001	0.050	0.004	0.032
Al	0.004	0.127	0.013	0.070	0.054	0.064
Fe	0.004	0.093	0.005	0.070	0.004	0.011
Mn	0.004	0.015	0.004	0.004	0.004	0.001
Mg	0.004	0.047	0.002	0.070	0.004	0.014
Ca	0.004	0.001	0.004	0.004	0.022	0.001
Na	0.004	0.015	0.004	0.030	0.056	0.072
K	0.004	0.002	0.004	0.040	0.002	0.074

The 8×14 A–B matrix has rank 8 and contains, without rank reduction, 2002 mass balances; 2002 is the result of:

$$\frac{m!}{(R!(m-R)!)},$$

where m and R are phases and rank of matrix. Each mass balance involves by definition $(R+1)$ phases, less than the full composite assemblage, and represents the linear combination of only $(m-R)$ independent relations, in the present case nine and six, respectively. Because of this combination process, groups of incompatibilites may show similar form and similar coefficients, in turn involving different phases, generally with low coefficients. As they may represent subreactions in the transition between samples, these incompatibilities can be combined to achieve an integrated mass balance that more closely approximates the actual reaction (Hartel & Pattison, 1996).

Allowing ilmenite to participate on either side of mass balance, and imposing Al_2SiO_5 as andalusite in B, 13 incompatibilities are found. Consequently, A and B intersect in composition space, and must have equilibrated under different external conditions. All incompatibilities have a similar form, with $Bt_A < Bt_B$, $Ms_A > Ms_B$, $Chl_A > Chl_B$, $St_A \geq St_B$, $Grt_A \geq Grt_B$; ilmenite is always present in A, and plagioclase is generally absent or present with small coefficients in either A or B. One of them (assemblage A on the left side) is

$$0.195\ \mathrm{St} + 1.414\ \mathrm{Chl} + 0.015\ \mathrm{Grt} + 5.000\ \mathrm{Ms} + 0.194\ \mathrm{Ilm} = 3.057\ \mathrm{And} + 0.150\mathrm{St} + 1.499\ \mathrm{Bt} + 3.775\ \mathrm{Ms} \quad (7)$$

Lang (1991) reduced such relations to 'net mass balances' by eliminating phases with similar compositions on opposite sides of the mass balance relation (Bt, St, Ms). This procedure is not strictly rigorous, because the phases are similar but not identical, and thus any information about exchange reactions is lost. However, such net balances may be useful as they are more similar to the usual notation of continuous reactions, providing easier monitoring of reactants, products and modal changes. In the case of mass balance (7), a reduction of this type leads to the net result

$$0.04\ \mathrm{St} + 1.41\ \mathrm{Chl} + 0.01\ \mathrm{Grt} + 1.23\ \mathrm{Ms} + 0.19\ \mathrm{Ilm} = 3.06\ \mathrm{And} + 1.50\ \mathrm{Bt} \quad (7a)$$

All the other net balances have similar coefficients for chlorite, andalusite, muscovite and biotite, with small, variable coefficients for staurolite, garnet and plagioclase. None of the incompatibilities in the composite matrix A–B contain both Al_2SiO_5 in B and $St_A < St_B$. On the other hand, if kyanite (abundant in A) is modelled as the Al_2SiO_5 polymorph, 21 St_B-forming $(St_A < St_B)$ incompatibilities are found, and all of them have $Grt_A > Grt_B$ and ilmenite in A. One is

$$4.579\ \mathrm{St} + 0.967\ \mathrm{Chl} + 0.520\ \mathrm{Grt} + 0.664\ \mathrm{Ms} + 0.141\ \mathrm{Ilm} + 1.256\ \mathrm{Ky} = 5.000\ \mathrm{St} + 0.633\ \mathrm{Bt} + 0.224\ \mathrm{Pl} \quad (8)$$

which has the net result

$$0.97\ \mathrm{Chl} + 0.52\ \mathrm{Grt} + 0.66\ \mathrm{Ms} + 0.14\ \mathrm{Ilm} + 1.26\ \mathrm{Ky} = 0.42\ \mathrm{St} + 0.63\ \mathrm{Bt} + 0.22\ \mathrm{Pl} \quad (8a)$$

and is similar in form (with different coefficients) to incompatibility (5) of matrix B.

Composite matrix B–C

The 8×14 B–C composite contains 2002 mass balances, of which 119 are incompatibilities. As most of them represent mass balances such as $Pl_B = Pl_C$ or $Ms_B = Ms_C$, only those that contain andalusite with fairly large coefficient (>0.7) and $Bt_B < Bt_C$ have been considered, because petrographic study indicates that these two minerals increase in amount in sample C. Of the 26 incompatibilities so found, all have $St_B \geq St_C$, $Chl_B \geq Chl_C$, $Grt_B \geq Grt_C$ and $Ms_B > Ms_C$; plagioclase is generally absent, or has a very low coefficient (≤ 0.1). Ilmenite can occur both in B or C. One group of incompatibilities is ilmenite- and plagioclase-free, and can be represented by the relation (B on the left side)

$$0.158\ \mathrm{St} + 4.265\ \mathrm{Bt} + 0.475\ \mathrm{Chl} + 0.069\ \mathrm{Grt} + 2.836\ \mathrm{Ms} = 3.047\ \mathrm{And} + 5.000\ \mathrm{Bt} + 0.023\ \mathrm{Grt} + 2.084\ \mathrm{Ms} \quad (9)$$

which has a net result

$$0.16\ \mathrm{St} + 0.47\ \mathrm{Chl} + 0.05\ \mathrm{Grt} + 0.75\mathrm{Ms} = 3.05\ \mathrm{And} + 0.73\ \mathrm{Bt} \quad (9a)$$

and is similar to (5a). A second group of similar relations has the model form:

$$0.164\ \mathrm{St} + 4.426\ \mathrm{Bt} + 0.562\ \mathrm{Chl} + 0.639\ \mathrm{Ms} + 0.039\ \mathrm{Ilm} = 2.839\ \mathrm{And} + 5.000\ \mathrm{Bt} + 0.216\ \mathrm{Chl} + 0.009\ \mathrm{Pl} \quad (10)$$

which has a net result

$$0.16\ \mathrm{St} + 0.35\ \mathrm{Chl} + 0.64\ \mathrm{Ms} + 0.04\ \mathrm{Ilm} = 2.84\ \mathrm{And} + 0.57\ \mathrm{Bt} + 0.01\ \mathrm{Pl} \quad (10a)$$

All these balances have similar net coefficients for biotite, chlorite and muscovite, small (<0.2) coefficients for staurolite and garnet, even smaller (<0.1) for plagioclase and ilmenite, and would correspond to the univariant tie-line break $\mathrm{St} + \mathrm{Chl} = \mathrm{And} + \mathrm{Bt}$ in the AFM system. They are similar to (9a) and also to (6) in the single matrix C, but have a much lower coefficient for plagioclase; as noted earlier, this difference may be related to the use of only one plagioclase composition in the single matrices, whereas the composites contain two of them and may better describe continuous chemical variations. Nine incompatibilities

contain ilmenite in C, such as

$$0.081\ \mathrm{St} + 0.300\ \mathrm{Chl} + 0.006\ \mathrm{Grt} + 0.025\ \mathrm{Pl} + 5.000\ \mathrm{Ms} = 0.096\ \mathrm{Ilm} + 1.300\ \mathrm{And} + 0.398\ \mathrm{Bt} + 4.706\ \mathrm{Ms} \quad (11)$$

which has a net result

$$0.08\ \mathrm{St} + 0.30\ \mathrm{Chl} + 0.01\ \mathrm{Grt} + 0.03\ \mathrm{Pl} + 0.29\ \mathrm{Ms} = 0.10\ \mathrm{Ilm} + 1.30\ \mathrm{And} + 0.40\ \mathrm{Bt} \quad (11a)$$

Compared to incompatibilities where ilmenite occurs in B, these have lower coeefficients for andalusite, biotite, chlorite and muscovite, and involve a lower amount of mass.

Composite matrix C–D

The 8×12 composite matrix C–D contains 220 mass balances, eight of which are incompatibilities. Four of them do not contain Al_2SiO_5 and have a very similar form, with ilmenite in C, $Ms_C > Ms_D$, $St_C < St_D$, $Bt_C < Bt_D$, and $Pl_C < Pl_D$. One is (C on the left side)

$$0.448\ \mathrm{Ilm} + 4.512\ \mathrm{St} + 0.855\ \mathrm{Chl} + 2.051\ \mathrm{Ms} + 0.837\ \mathrm{Grt} = 5.000\ \mathrm{St} + 1.574\ \mathrm{Bt} + 0.912\ \mathrm{Pl} + 0.062\ \mathrm{Ms} \quad (12)$$

The net result of this incompatibility can be expressed as

$$0.45\ \mathrm{Ilm} + 1.99\ \mathrm{Ms} + 0.86\ \mathrm{Chl} + 0.84\ \mathrm{Grt} = 0.49\ \mathrm{St} + 1.57\ \mathrm{Bt} + 0.91\ \mathrm{Pl} \quad (12a)$$

where the coefficients refer to the particular case of (12), and differ only slightly in the other mass balances. Two incompatibilities contain Al_2SiO_5 on the D side, such as

$$0.581\ \mathrm{Ilm} + 4.915\ \mathrm{St} + 2.562\ \mathrm{Bt} + 0.832\ \mathrm{Grt} + 1.557\ \mathrm{Ms} = 5.000\ \mathrm{St} + 1.816\ \mathrm{Sil} + 3.695\ \mathrm{Bt} + 0.899\ \mathrm{Pl} \quad (13)$$

which has the net form

$$0.58\ \mathrm{Ilm} + 0.83\ \mathrm{Grt} + 1.56\ \mathrm{Ms} = 1.82\ \mathrm{Sil} + 0.09\ \mathrm{St} + 1.13\ \mathrm{Bt} + 0.90\ \mathrm{Pl} \quad (13a)$$

Two other incompatibilities contain Al_2SiO_5 on the C side, such as

$$0.105\ \mathrm{Ilm} + 2.338\ \mathrm{St} + 5.000\ \mathrm{And} + 2.482\ \mathrm{Pl} + 0.566\ \mathrm{Grt} + 0.166\ \mathrm{Ms} = 2.965\ \mathrm{St} + 0.133\ \mathrm{Bt} + 2.671\ \mathrm{Pl} \quad (14)$$

which has the net form

$$0.11\ \mathrm{Ilm} + 5.00\ \mathrm{And} + 0.57\ \mathrm{Grt} + 0.17\ \mathrm{Ms} = 0.63\ \mathrm{St} + 0.13\ \mathrm{Bt} + 0.19\ \mathrm{Pl} \quad (14a)$$

All these relations indicate that C and D intersect in composition space, but do not help to constrain the evolution between assemblages. In fact, all contain $St_C < St_D$ and would imply a net increase of staurolite in sample D, the opposite of textural evidence.

DISCUSSION

The approach undertaken in this study differs from that of other analyses (e.g. Giaramita & Day, 1991; Lang, 1991), where within-outcrop variations were investigated to understand whether differences in assemblages could relate to changes in bulk composition or in metamorphic conditions. In the present case, the four samples are distributed along a 1 km traverse, and differ either weakly or significantly in contact metamorphic grade. It is apparent that their external conditions of equilibration (i.e. temperature) were different and are responsible, at least in part, for the changes in mineral assemblages. Exploration of mass balances is used here to analyse the compositional and reaction relationships among samples.

Bulk composition relationships

Based on the microstructures observed in samples A–D, interpreted as stages in a sequence of pseudomorphs after garnet, and on the fact that these textures only occur in the rock layers where the samples were collected, Cesare (1999) proposed that the samples belong to a common rock type. The similarity of normalized oxide values is an argument in favour of such hypothesis: in fact, from a graphical point of view, it can be observed that in the model KFMASH system (Fig. 2) all bulk compositions nearly overlap in the small intersection volume common to all assemblages. Exploration of bulk composition relationships in the full multi-component system has also been approached by matrix analysis. Because the existence of incompatibilities in the composites implies intersection of assemblages, the samples belong to different mineral facies. However, this does not tell us much about bulk composition relationships, which can lie anywhere within the space defined by their assemblages, and still be very different; likewise in the compatibility situation. What incompatibilities tell is that assemblages *may* be similar (or even equal), i.e. lie in the intersection of assemblage spaces. To verify whether bulk compositions lie in the intersection volume in the full Ca–Na–Mn–Ti–KFMASH system, one should compare each assemblage with the remaining three bulk compositions (i.e. analyse the 12 composite matrices $\mathrm{assemblage}_{\mathrm{sample}=i} + \mathrm{bulk}_{\mathrm{sample}\neq i}$) and always find incompatibilities. It turns out that no incompatibilities exist among assemblages and compositions of other samples (e.g. $\mathrm{assemblage}_A + \mathrm{bulk}_B$), implying that the samples do not lie in the intersection of assemblages in the full multi-component system. However, it was also found that no incompatibilities exist between assemblage C and its own bulk composition, which would suggest that the bulk composition lies outside the space defined by the assemblage. As this is impossible, the most plausible reason is that the measured compositions are not fully representative of the chemical variations of phases (because of zoned

minerals such as garnet and plagioclase), and that the estimated errors are not able to correct for this incompleteness. Another explanation is that the rocks are not homogeneous.

Thus it can be concluded that the study samples are not identical, but are very similar, at least as far as the model pelitic system is considered, and that non-AFM components account for the departure of bulk compositions from the compositional volume defined by intersection of AFM assemblages. Among the non-AFM components, Na_2O has the largest relative variations (Table 3), with sample D showing a very low value. A possible explanation, other than a primary difference, for the low Na_2O content of D may be syn-metamorphic Na depletion by base-cation leaching (Vernon, 1987). This is supported by the occurrence of dissolution textures involving quartz and plagioclase along high-strain zones abutting fibrolite-rich folia (Cesare, 1999). In this case, the low Na_2O content of sample D would represent an inherited characteristic that does not reflect the primary compositional relationships among samples.

Reaction relationships

Reaction relationships can be approached by matrix analysis of both single and composite matrices: mass balances identified in single matrices can indicate either disequilibrium relationships or univariant reactions; on the other hand, incompatibilities in a composite matrix may represent the actual reactions changing one facies assemblage into the other. As noted by Greenwood (1967), 'reactions so deduced are ordinarily not stable reactions, and are likely to include in one step a number of stable and metastable steps'. Nonetheless, the importance of mass balances determined by matrix analysis is not diminished, as these are able to describe the chemical changes occurring in the transition from two metamorphic facies, disregarding how the conditions defining them (*P*, *T*, chemical potentials) have changed. Thus, combining information from single and composite matrices can help to reconstruct how the different assemblages developed and whether they may have derived from one another. This approach is also helpful in verifying the validity of mass balances such as (4) and (6) that resulted from uncertain models.

Samples A and B contain phases (Ky & Grt) that are in clear textural disequilibrium. The incompatibilities in the single matrices reflect this situation and the fact that kyanite and garnet are reactant in staurolite-forming reactions such as (3) and (5). Mass balances (4) and (6) in the single matrices B and C provide information on andalusite formation, indicating expansion of the AFM relationship $St + Chl = Bt + And$ to a more complex 10-component system. In the case of matrix C, incompatibility (6) was shown to result from a questionable model. However, its similarity to (9) and (10) in the composite B–C supports the conclusion that it represents more than a simple mass balance equation, and can be accepted as a good approximation to the reaction occurring in sample C.

The absence of mass balances in the single matrix D indicates that no reaction relationships exist, because the assemblage occupies a divariant field in compositional space. With regard to the composite C–D, all the incompatibilities would suggest consumption of muscovite and ilmenite ($\pm Chl \pm Grt$), and growth of biotite, plagioclase and staurolite. As the latter indication is not consistent with petrographic evidence of staurolite dissolution, these incompatibilities (or any combination of them) cannot represent the transition between samples C and D. Thus, reaction (2) inferred from the basis of textural evidence could not be verified by matrix analysis.

Andalusite–staurolite relationships in samples B and C

A problem arising from textural analysis of sample B was whether andalusite and staurolite could have grown at the same time, in contrast with the theoretical behaviour of the model pelitic system (e.g. Thompson, 1976) which predicts that staurolite should be reactant for the growth of biotite and andalusite. Mass balances in the single matrices B and C, and incompatibilites in the composite B–C have two general forms: on one hand the kyanite-consuming, staurolite-producing reaction (5); on the other hand the andalusite-producing, staurolite-consuming reactions (4), (6), (9) or (10). Because the B–C matrix could not account for the Ky→And transition, for a reaction to be meaningful both Al_2SiO_5 polymorphs have to be present, one on each side. Combining the two types of incompatibilities reveals interesting information on the behaviour of staurolite in these rocks. If (4) and (5) are added together, the resulting relation has the net form

$$Ky + Ilm + Chl + Grt + Ms = And + St + Bt + Pl \quad (15)$$

and indicates that the staurolite produced by the kyanite-consuming reaction is more than the staurolite required by andalusite production. Such a combined mass balance confirms the possibility that staurolite and andalusite grew at the same time in sample B, and the textural observations of Cesare (1999) who proposed the AFM reaction (1) as the transition between A and C. Because at least one metastable phase (Ky) is involved, these relations do not represent equilibrium reactions nor the final stage of equilibration of the And–St–Bt assemblage. The latter can be evaluated by analysis of incompatibilities in the single matrix C, where kyanite does not occur. Relationships such as (6) indicate that, after kyanite disappearance, andalusite growth occurs via staurolite consumption, e.g. that in the final stages of equilibration, staurolite is a reactant.

Ionic reaction cycles during development of assemblage D

Based on the modal changes observed between C and D, namely on the consumption of staurolite and chlorite, decrease of muscovite, and increase of biotite and sillimanite, reaction (2) was proposed as a possible model for the prograde evolution from C to D. This reaction is in contrast with the textural evidence of muscovite growth after staurolite in the nodules of sample D. Such seeming inconsistency could be explained if (2) or any other reaction linking the two samples occurred via an ionic reaction mechanism (Carmichael, 1969), in which simultaneous subreactions take place in the different domains of the rock. In this perspective, muscovite is consumed in the matrix, whereas is produced in the nodules, in such a way that the net balance is consumption.

All the incompatibilities found in the composite matrix C–D contain $Ms_C > Ms_D$, and support the occurrence of a muscovite-consuming net reaction such as (2). This implies that even if this phase grows in the nodules of sample D, a larger amount must have dissolved in the adjacent matrix. It can be concluded that matrix analysis of assemblages agrees with microstructural evidence for redistribution of minerals in the rock in a manner that compares to the reaction mechanism proposed by Carmichael (1969). In this way, prograde pseudomorphs of muscovite after staurolite can occur even in the case of net consumption of both phases.

CONCLUSIONS

This work highlights both the effectiveness and the limits of the matrix analysis approach in modelling mineral reactions. As calculated mass balances contain by definition $R+1$ phases, a unique solution to the problem of calculating a balanced univariant reaction can only be obtained with matrices where $R=m-1$. This condition is easier to obtain with single matrices, as in samples A, B and C, although single matrices may suffer from the problem of fully describing the chemical features of the system and phases, especially when dealing with zoned minerals. Incomplete information on chemical composition of phases may result in questionable models and unreliable mass balances that can be corrected by use of alternative methods such incorporation of exchange vectors (e.g. Hartel & Pattison, 1996). Composite matrices generally have an excess number of phases, so that the incompatibilities do not relate all phases from each sample and in most cases provide only information on the possible intersection in composition space. In this case, inspection of mass balances for systematic patterns (e.g. the coherent behaviour of staurolite, chlorite, garnet and muscovite in the composite B–C) can provide qualitative information on the first-order general form of reaction(s). Furthermore various forms of combination of incompatibilities may result in mass balances relating most or all phases in the composite, and in closer approximation to the observed textures. However, these methods will not result in the definition of a unique reaction, which can only be retrieved if samples share a common, known, bulk composition.

ACKNOWLEDGEMENTS

Many thanks to G. Fisher for providing the matrix analysis programs, reading the manuscript and discussing the general aspects of assemblage investigation, and to M. Ballèvre, J. Connolly and M. Guiraud for their comments. Thorough reviews by D. Pattison and C. DeBuhr pointed out some important conceptual errors and are particularly acknowledged. The patient editorial handling by D. Robinson was also very much appreciated. Financial support from MURST and CNR. Support for microprobe analysis at the IMP-ETH, Zürich.

REFERENCES

Bellieni, G., Peccerillo, A. & Poli, G., 1981. The Vedrette di Ries (Rieserferner) plutonic complex: petrological and geochemical data bearing on its genesis. *Contributions to Mineralogy and Petrology*, **78,** 145–156.

Borsi, S., Del Moro, A., Sassi, F. & Zirpoli, G., 1973. Metamorphic evolution of the Austridic rocks to the south of the Tauern window (Eastern Alps). Radiometric and geopetrologic data. *Memorie della Società Geologica Italiana*, **12,** 549–571.

Carmichael, D. M., 1969. On the mechanism of prograde metamorphic reactions in quartz-bearing pelitic rocks. *Contributions to Mineralogy and Petrology*, **20,** 244–267.

Cesare, B., 1999. Multi-stage pseudomorphic replacement of garnet during polymetamorphism: microstructures and their interpretation. *Journal of Metamorphic Geology*, **19,** 727–737.

Fisher, G. W., 1989. Matrix analysis of metamorphic mineral assemblages and reactions. *Contributions to Mineralogy and Petrology*, **102,** 69–77.

Fisher, G. W., 1990. The exploration of reaction space. In: *Fluid–Mineral Interactions: a Tribute to H.P. Eugster* (eds Spencer, R. J. & Chou, I.-m.). *Geochemical Society Special Publications*, **2,** 133–139.

Fletcher, C. J. N. & Greenwood, H. J., 1979. Metamorphism and structure of Penfold Creek area, near Quesnel Lake, British Columbia. *Journal of Petrology*, **20,** 743–794.

Giaramita, M. J. & Day, H. W., 1991. Buffering of H_2O in staurolite–aluminium silicate–biotite–garnet–chlorite assemblages. *Journal of Metamorphic Geology*, **9,** 363–378.

Gordon, T. M., Ghent, E. D. & Stout, M. Z., 1991. Algebraic analysis of the biotite–sillimanite isograd in the File Lake area, Manitoba. *Canadian Mineralogist*, **29,** 673–686.

Greenwood, H. J., 1967. The N-dimensional tie-line problem. *Geochimica et Cosmochimica Acta*, **31,** 465–490.

Guidotti, C. V., 1970. The mineralogy and petrology of the transition from the lower to upper sillimanite zone in the Oquossoc area, Maine. *Journal of Petrology*, **11,** 277–336.

Hartel, T. H. D. & Pattison, D. R. M., 1996. Genesis of the Kapuskasing (Ontario) migmatitic mafic granulites by dehydration melting of amphibolite: the importance of quartz to reaction progress. *Journal of Metamorphic Geology*, **14,** 591–611.

Lang, H. L., 1991. Quantitative interpretation of within-outcrop variation in metamorphic assemblage in staurolite-kyanite-grade metapelites, Baltimore, Maryland. *Canadian Mineralogist*, **29,** 655–671.

Lang, H. M. & Rice, J. M., 1985. Regression modelling of

metamorphic reactions in metapelites, Snow Peak, northern Idaho. *Journal of Petrology*, **26,** 857–887.

Pattison, D. R. M., 1987. Variations in Mg/(Mg + Fe), F, and (Fe,Mg)Si = 2 Al in pelitic minerals in the Ballachulish thermal aureole, Scotland. *American Mineralogist*, **72,** 255–272.

Pigage, L. C., 1982. Linear regression analysis of sillimanite-forming reactions at Azure Lake, British Columbia. *Canadian Mineralogist*, **20,** 349–378.

Powell, R., 1990. Matrix analysis of metamorphic mineral assemblages and reactions: alternatives and extensions. *Contributions to Mineralogy and Petrology*, **106,** 61–65.

Thompson, J. B., 1957. The graphical analysis of mineral assemblages in pelitic schists. *American Mineralogist*, **42,** 842–858.

Thompson, A. B., 1976. Mineral reactions in pelitic rocks: I. Prediction of *P–T–X* (Fe–Mg) phase relations. *American Journal of Science*, **276,** 401–424.

Tuisku, P., Ruostesuo, P. & Häkkinen, A., 1987. The metamorphic behaviour and petrogenetic significance of zinc in amphibolite facies, staurolite-bearing mica schists, Puolankajärvi Formation, Central Finland. *Geochimica et Cosmochimica Acta*, **51,** 1639–1650.

Vernon, R. H., 1987. Growth and concentration of fibrous sillimanite related to heterogeneous deformation in K-feldspar–sillimanite metapelites. *Journal of Metamorphic Geology*, **5,** 57–68.

Received 26 November 1997; revision accepted 7 June 1999.